ACCOUNTS of chemical research

Article

pubs.acs.org/accounts

Surface-Activated Coupling Reactions Confined on a Surface

Published as part of the Accounts of Chemical Research special issue "Microscopic Insights into Surface Catalyzed Chemical Reactions".

Lei Dong,[†] Pei Nian Liu,*[,‡] and Nian Lin*[,†]

[†]Department of Physics, The Hong Kong University of Science and Technology, Clear Water Bay, Hong Kong, China

[‡]Shanghai Key Laboratory of Functional Materials Chemistry, Key Lab for Advanced Materials and Institute of Fine Chemicals, East China University of Science and Technology, Meilong Road 130, Shanghai 200237, China

CONSPECTUS: Chemical reactions may take place in a pure phase of gas or liquid or at the interface of two phases (gas–solid or liquid–solid). Recently, the emerging field of "surface-confined coupling reactions" has attracted intensive attention. In this process, reactants, intermediates, and products of a coupling reaction are adsorbed on a solid–vacuum or a solid–liquid interface. The solid surface restricts all reaction steps on the interface, in other words, the reaction takes place within a lower-dimensional, for example, two-dimensional, space. Surface atoms that are fixed in the surface and adatoms that move on the surface often activate the surface-confined coupling reactions. The synergy of surface morphology and activity allow some reactions that are inefficient or prohibited in the gas or liquid phase to proceed efficiently when the reactions are confined on a surface. Over the past decade, dozens of well-known "textbook" coupling reactions have been shown to proceed as surface-confined coupling reactions.

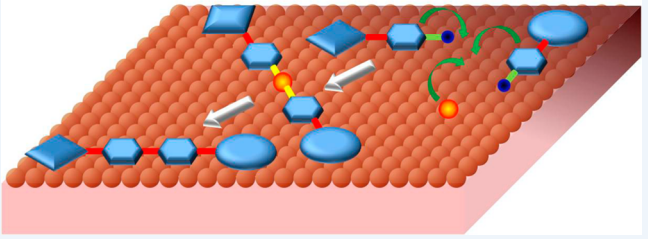

In most cases, the surface-confined coupling reactions were discovered by trial and error, and the reaction pathways are largely unknown. It is thus highly desirable to unravel the mechanisms, mechanisms of surface activation in particular, of the surface-confined coupling reactions. Because the reactions take place on surfaces, advanced surface science techniques can be applied to study the surface-confined coupling reactions. Among them, scanning tunneling microscopy (STM) and X-ray photoelectron spectroscopy (XPS) are the two most extensively used experimental tools. The former resolves submolecular structures of individual reactants, intermediates, and products in real space, while the latter monitors the chemical states during the reactions in real time. Combination of the two methods provides unprecedented spatial and temporal information on the reaction pathways. The experimental findings are complemented by theoretical modeling. In particular, density-functional theory (DFT) transition-state calculations have been used to shed light on reaction mechanisms and to unravel the trends of different surface materials.

In this Account, we discuss recent progress made in two widely studied surface-confined coupling reactions, aryl–aryl (Ullmann-type) coupling and alkyne–alkyne (Glaser-type) coupling, and focus on surface activation effects. Combined experimental and theoretical studies on the same reactions taking place on different metal surfaces have clearly demonstrated that different surfaces not only reduce the reaction barrier differently and render different reaction pathways but also control the morphology of the reaction products and, to some degree, select the reaction products. We end the Account with a list of questions to be addressed in the future. Satisfactorily answering these questions may lead to using the surface-confined coupling reactions to synthesize predefined products with high yield.

1. INTRODUCTION

In homogeneous catalysis, reactants, products, and catalysts are in the same phase (liquid or gas); in heterogeneous catalysis, reactions take place at solid–liquid or solid–gas interfaces (Scheme 1). In surface-confined coupling reactions, surface atoms, intrinsic or foreign adatoms moving on the surface, bear the characteristics of both homogeneous and heterogeneous catalysis. As illustrated in Scheme 1, in a surface-confined coupling reaction, reactants, products, and intermediates (if any) are mixed and free to move yet remain adsorbed on a solid surface; namely, the reactions are restricted within a two-dimensional (2D) space. Surface atoms, surface defects (steps and kinks), intrinsic adatoms that pop out of the surface, or foreign atoms or clusters deposited on the surface may activate or catalyze the reactions. Because the reactants are adsorbed on the surface in specific conformation and orientation, the surface-confined coupling reactions may be sterically enhanced or hindered compared with the counterpart reactions taking place in a three-dimensional space. As a result, the surface-confined coupling reactions often exhibit unique features, such as regio- and stereoselectivity, easily accessible active sites, and thermotolerance. These characteristics resemble heterogeneous catalytic reactions. However, the surface-confined coupling

Received: March 30, 2015
Published: August 28, 2015

ACS Publications © 2015 American Chemical Society

DOI: 10.1021/acs.accounts.5b00160
Acc. Chem. Res. 2015, 48, 2765–2774

Scheme 1. Comparison of Homogeneous, Heterogeneous Catalysis, and Surface-Confined Coupling Reactions

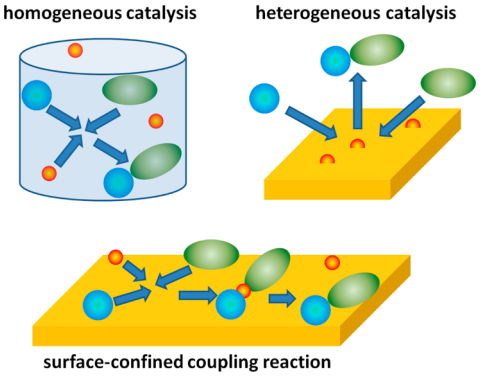

reactions differ from heterogeneous catalytic reactions by nature since the catalysts and the reactants are mixed in the same phase of a 2D space. In this regard, the surface-confined coupling reactions can be viewed as homogeneous reactions taking place in 2D. Another feature of the surface-confined coupling reactions is that advanced techniques of surface science, including microscopy and spectroscopy characterization tools under well-defined conditions of cryogenic temperature and ultrahigh vacuum (UHV), and theoretical tools of atomistic modeling, can be employed to analyze reactants, intermediates, and products, as well as reaction steps. These techniques provide unprecedented insights of the reactions in great details, which afford a deep understanding of the reaction mechanism.

In less than 10 years, surface-confined coupling reactions have been developed to generate a wide range of organic systems, including macromolecules, polymeric chains, two-dimensional porous organic networks, graphene nanoribbons, and super honeycomb networks, etc. Various well-known organic reactions have been shown to work well in an surface-confined setting, including aryl−aryl coupling (Ullmann-type reaction), alkyne (Glaser-type reaction) coupling, condensation reactions of boronic acids,[1−3] imine formation,[4] dimerization of N-heterocyclic carbenes,[5] alkane polymerization,[6] acylation reactions,[7,8] Bergman cyclization,[9] cyclodehydrogenation,[10,11] click reactions,[12] and cycloaddition reactions.[12,13] In many aspects, the surface-confined coupling reactions resemble the counterpart reactions in solution; nevertheless, the reaction pathways and products often vary significantly on different surfaces, indicating that the surfaces play critical roles. In this Account, we examine *in vacuo* surface-confined Ullmann-type and Glaser-type coupling, and we focus on surface activity. More comprehensive reviews of surface-confined coupling reactions can be found elsewhere.[14−17]

2. ARYL−ARYL (ULLMANN-TYPE) COUPLING

In 1901, Fritz Ullmann discovered a reaction that fused two halogen aryl moieties into a biphenyl with the help of a copper powder.[18] This reaction, which became known as the classical Ullmann reaction, has been extensively used in organic synthesis.[19] In 1992, Xi and Bent reported surface-confined Ullmann reaction in UHV for the first time.[20,21] In 2000, Hla et al. used a scanning tunneling microscope (STM) tip to manipulate two iodobenzene molecules on a Cu(111) surface at liquid helium temperature to form a biphenyl molecule.[22] In 2007, a seminal work by Grill et al. demonstrated that brominated porphyrin derivatives spontaneously linked via Ullmann coupling to form macromolecular and oligomeric

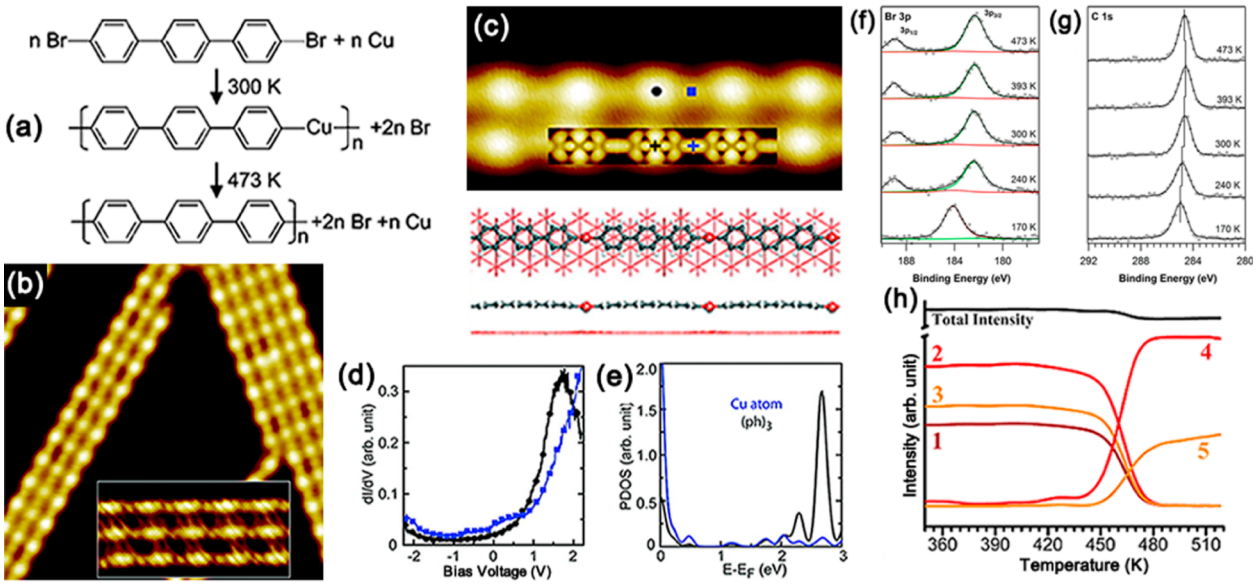

Figure 1. (a) The pathway of surface-confined Ullmann coupling of 4,4′-dibromo-*p*-terphenyl on Cu(111). (b) STM image of the sample annealed at 300 K (20 × 20 nm^2). Inset: Br atoms lying between the linear structures (8 × 4 nm^2). (c) High-resolution STM image of the intermediate (8 × 4 nm^2) and the DFT-calculated structure. Inset: DFT-simulated STM image at +2.7 V. (d) d*I*/d*V* spectra measured at terphenyl (black) and Cu (blue) marked in panel c. (e) Calculated PDOS of terphenyl (black) and Cu (blue). Reproduced with permission from ref 24. Copyright 2011 American Chemical Society. (f) Br 3p and (g) C 1s XP spectra of TBPB on Cu(111) with a coverage of θ = 0.027 (around 0.9 monolayers). TBPB was deposited onto Cu(111) with the substrate held at 170 K. Reproduced with permission from ref 33. Copyright 2014 American Chemical Society. (h) Intensity functions of C 1s core levels as a function of annealing temperature acquired by fast-XPS measurement. One is assigned to carbon bound to copper, 2 and 3 are assigned to the dehalogenated phenyl molecules, and 4 and 5 are assigned to the coupled carbon. Reproduced with permission from ref 45. Copyright 2013 American Chemical Society.

DOI: 10.1021/acs.accounts.5b00160
Acc. Chem. Res. 2015, 48, 2765−2774

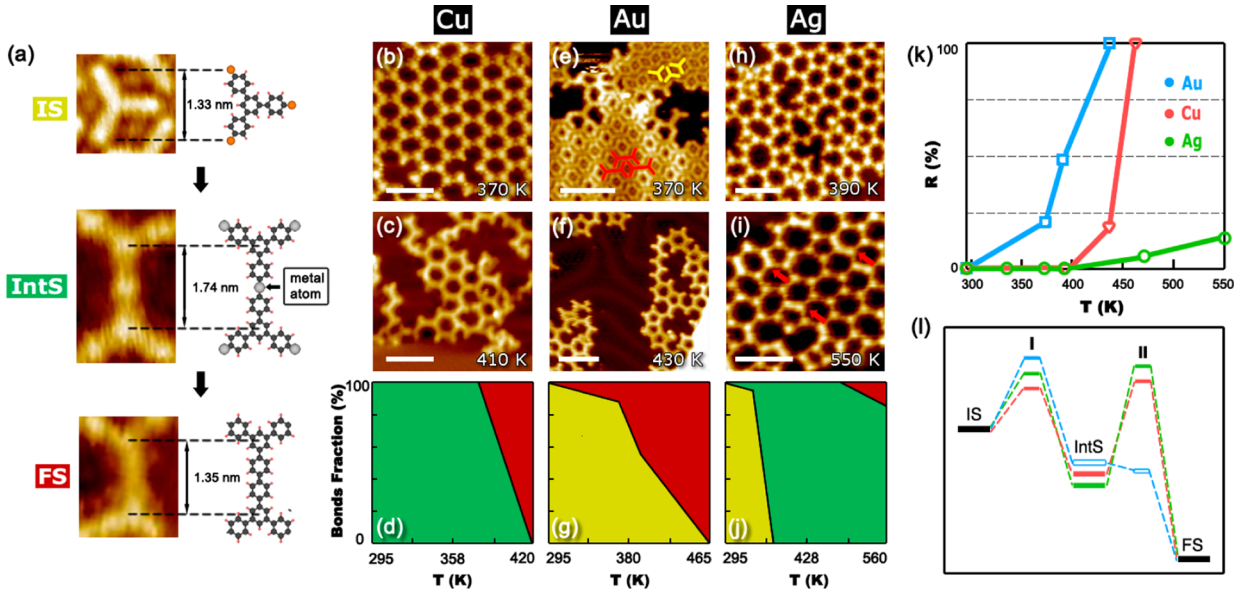

Figure 2. (a) STM topographs and models of the initial state (**IS**), Ag organometallic intermediate state (**IntS**), and final state (**FS**). (b–j) STM images of representative structures and the bonds fraction during the reaction process on Cu (b–d), Au (e–g,) or Ag (h–j). **IS**, **IntS**, and **FS** are represented in yellow, green and red, respectively. Scale bar: 5 nm. (k) Conversion ratios (*R*) as a function of annealing temperatures of the Ullmann coupling on these surfaces. (l) Schematic energy diagram of Ullmann coupling on (111) surfaces of Cu, Au, and Ag [ref 47].

structures on Au(111).[23] Since then, this reaction has been used to generate various covalently linked molecular systems out of different halogen aryl moieties on different metal surfaces. The reaction has been studied using a wide range of advanced surface science techniques, including high-resolution electron energy loss spectroscopy (HREELS),[20,21] STM,[24−32] H/D atom titration,[20,21] temperature-programmed reaction (TPR),[20,21] X-ray photon spectroscopy (XPS),[33−35] and near-edge X-ray absorption fine structure spectroscopy (NEXAFS).[36] These studies have revealed some key aspects of the surface-confined Ullmann coupling reaction, leading to the conclusion that the surfaces effectively activate the reaction. In the following sections, we compare the surface-confined Ullmann reaction on Cu(111), Au(111), and Ag(111) surfaces. We focus on two roles the surfaces play: (1) forming the organometallic intermediate and (2) activating the reaction. We also discuss the surface-confined Ullmann-type reaction activated by *extrinsic* Cu, Pd, and Pt as deposits on a surface.

2.1. Organometallic Intermediate

The generally accepted mechanism for the Ullmann reaction involves multiple steps including (1) formation of an organocuprate intermediate from a molecule containing an aryl halide moiety, (2) oxidative addition with another molecule, and (3) reductive elimination toward the final product.[37,38] However, the actual intermediate is still under debate. In the surface-confined Ullmann reaction, different intermediates have been proposed.[39−42] Xi and Bent[20,21] and Blake et al.[27] proposed that 1,4-iodobenzene molecules form a protopolymer on Cu(111) that features a surface-mediated interaction between dehalogenated phenyl moieties and the surface atoms. The same surface-mediated structures were observed by Lipton-Duffin et al. on Cu(110) and by Lewis et al. on Co islands.[40,43] Walch et al. reported a different intermediate structure formed by a larger polyphenyl molecule, 1,3,5-tris(4-bromophenyl)benzene (TBPB), on Cu(111) and Ag(111).[25] Based on intermolecular distances resolved in STM topographs, those authors proposed that the intermediate is an aryl−metal−aryl coordination complex in which the metal atom is an adatom that sits in the same plane as the aryl moieties. Similar structure has been reported in an anthryl−Ag−anthryl system.[44]

Wang et al. characterized the reactants, intermediates, and products in the Ullmann coupling reaction of 4,4′-dibromo-*p*-terphenyl on Cu(111) (Figure 1a).[24] Using STM and density-functional theory (DFT) modeling, they showed that the intermediate structure, which forms at an intermediate temperature, consists of large, bright ovals and small, dim dots in a periodic chain arrangement (Figure 1b,c). The ovals are terphenyl moieties and the dots are Cu adatoms. A DFT-optimized structure is shown below the STM image in Figure 1c. The side view reveals that the Cu atoms lie nearly coplanar with the terphenyl moieties and that each Cu atom forms two C−Cu bonds (C−Cu = 2.11 Å) with the neighboring terphenyl units. Tunneling (dI/dV) spectra (Figure 1d) show that the terphenyl features a prominent peak at +1.7 V, whereas the Cu atom features a gradually rising intensity. The calculated projected density of states (PDOS) of the terphenyl (Figure 2e) exhibits a sharp peak at +2.7 V, while the Cu adatom has no apparent features. The calculated PDOS is in fair agreement with experimental dI/dV spectra. The inset in Figure 1c shows a simulated STM image of the intermediate structure at +2.7 V. It reproduces the main features of the experimental STM image. The intermediate structure was found to convert to the final products of polyphenylene chains at 470 K. Similar intermediate of an Ag-bridged structure on Ag(111) surface was reported by Chung et al.[28]

Chen et al. studied the adsorption and reaction of TBPB on Cu(111) surface using XPS.[33] The molecules were vapor deposited onto Cu(111) at a sample temperature of 170 K. Br 3p and C 1s XP spectra were taken at 170 K and higher temperatures. At 170 K, the Br $3p_{3/2}$ signal consists of a single peak at 184.1 eV, as shown in Figure 1f, which is associated with intact TBPB. Once the sample was heated to 240 K, the original Br $3p_{3/2}$ peak at 184.1 eV was nearly fully converted

DOI: 10.1021/acs.accounts.5b00160
Acc. Chem. Res. 2015, 48, 2765−2774

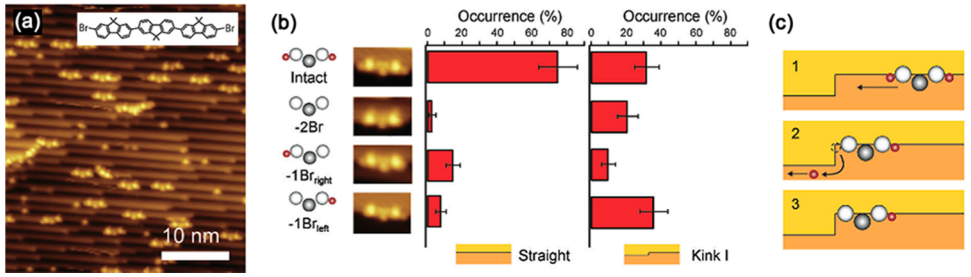

Figure 3. (a) Dibromoterfluorene (DBTF) adsorbed on a stepped Au(10,7,7) surface. (b) Relative frequencies of different types of Br removal from DBTF molecules adsorbed at straight step edges or kink I sites on an Au(10,7,7) surface. (c) Proposed kink catalysis. Reproduced with permission from ref 50. Copyright 2012 Wiley-VCH.

into a peak at 182.4 eV. No significant changes were observed after heating to higher temperatures of up to 473 K, indicating that the C−Br bond scission is complete by 240 K. A single C 1s peak appears at 285.0 eV, as shown in Figure 1g. This peak shifts gradually to lower binding energy with increasing temperature up to 393 K. From 393 to 473 K, the peak shifts slightly back to higher binding energy.

Di Giovannantonio et al. used fast-XPS to monitor the dynamic transition from an organometallic intermediate structure to covalently bonded polymers.[45] They demonstrated how temperature controlled the evolution of the organometallic intermediate state in Ullmann coupling of 1,4-dibromobenzene on a Cu(110) surface. Spectral analysis confirmed that debromination was complete at room temperature and the C 1s core level peak at 283.2 eV was assigned to C−Cu binding, supporting the interpretation that an organometallic intermediate incorporating C−Cu bonds forms at room temperature. Analysis of the peak intensities of the C 1s state as a function of annealing temperature (Figure 1h) suggests that the vanishing of the peak at 283.2 eV can be considered the limiting step for the conversion into covalent bonding. The transition temperature is estimated to be 460 ± 10 K, which confirms the picture proposed in ref 24.

The behavior of the intermediate state differs on different metal surfaces. Figure 2 compares Ullmann coupling of TBPB molecules on Cu(111), Au(111), and Ag(111). Three states, the initial state of intact molecules (**IS**), the intermediate state featuring an organometallic intermediate (**IntS**), and the final state featuring covalently linked molecules (**FS**) can be resolved in STM topograph shown in Figure 2a. On Cu(111), the transition from **IS** to **IntS** occurs in the temperature range of 170 to 240 K.[33] Annealing to 370 K caused the **IntS** to develop into larger and regular organometallic networks (Figure 2b), indicating that the C−Cu−C bonds are quite stable at this temperature. Further annealing to 390 K disrupted the regular networks of **IntS**, converting a small fraction of it into **FS**. Conversion of **IntS** to **FS** became significant above 400 K and reached more than 90% at 410 K (Figure 2c). On Ag(111), the transition from **IS** to **IntS** occurred at 390 K.[44] Annealing to 550 K converted only 10% of **IntS** into **FS** (marked by the red arrows in Figure 2i), indicating that the **IntS** was quite robust against annealing on Ag(111). On Au(111), covalently coupled dimers formed at ∼380 K (Figure 2e).[29,46] Further annealing to 430 K led to irregular polymer network structures associated with the molecules fully converted to **FS** (Figure 2f). In sharp contrast to the Cu and Ag surfaces, no **IntS** was observed on Au(111).

2.2. Intrinsic Substrate Activation

The temperature-dependent evolution of **IS**, **IntS**, and **FS** in the Ullmann coupling on the three surfaces is plotted in Figure 2d,g,j. These graphs suggest that the Ullmann reaction proceeds differently on the three surfaces.[47] For example, **IS** is present on Au(111) and Ag(111) at 295 K but not on Cu(111), indicating that the **IS** is stable on Au and Ag but more easily activated on Cu. **IntS** forms on Cu and Ag but not on Au, suggesting that C−Au−C is either unstable or has a short lifetime. On Cu or Au, all molecules convert to **FS** at 420 or 465 K, but on Ag the conversion is only about 10% even at 560 K.[48] The overall reaction yields on the three surfaces, defined as the ratio of **FS** to **IS**, are plotted in Figure 2k. One can see that the coupling takes place at 300 and 400 K and completes at 420 and 465 K on Au(111) and Cu(111), respectively. On Ag(111), the reaction starts at the same temperature of 400 K as it does on Cu(111) but increase much more slowly than it does on Cu(111) with temperature increment. In conclusion, surface activation efficiency is in the order of Au(111) > Cu(111) > Ag(111). These differences are rationalized in a qualitative energy diagram (Figure 2l), which features an energy barrier I that defines conversion of **IS** to **IntS** and a barrier II that defines conversion of **IntS** to **FS**. It is worthwhile to point out different orientations of the same material, for example, Cu(111) and Cu(110), exhibit quite different activity.[49]

2.3. Kink Activation

Defects such as step edges and kinks on catalytic surfaces are thought to serve as "active sites" in heterogeneous catalytic reactions. Saywell et al. investigated the activation effect of kink sites on a stepped Au(10,7,7) surface for the surface-confined Ullmann-type coupling.[50] The Au(10,7,7) surface has a misorientation angle of ∼9° to Au(111) and thus shows narrow (111)-oriented terraces separated by step edges with kinks facing the right side (Figure 3a). On this surface, dibromoterfluorene (DBTF) molecules adsorbed in two characteristic adsorption geometries: One is parallel to the step on the straight region of the steps, while the other shows an approximately 10° tilt at the kink sites. Most molecules (75%) at straight steps remained intact, and in those (25%) that underwent debromination, the dissociation of Br atoms happened equally at either of the two termini (Figure 3b). In comparison, the fraction of debrominated molecules was doubled at kink sites, and 95% of Br atoms were removed from the left terminus compared with only 5% from the right terminus, in accordance with the right-side facing kinks. These results led Saywell et al. to propose the mechanism depicted in Figure 3c. Intact DBTF molecules diffuse along the straight step edge, and the Br atoms at the termini are catalytically

DOI: 10.1021/acs.accounts.5b00160
Acc. Chem. Res. 2015, 48, 2765−2774

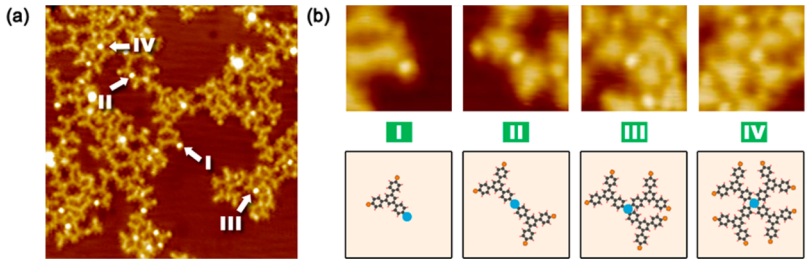

Figure 4. (a) STM image (25.4 × 25.4 nm^2) of the intermediate structures formed by Pt and TBPB. (b) STM images (3.2 × 3.2 nm^2) showing the structures of different coordination numbers and the corresponding structural models [ref 47].

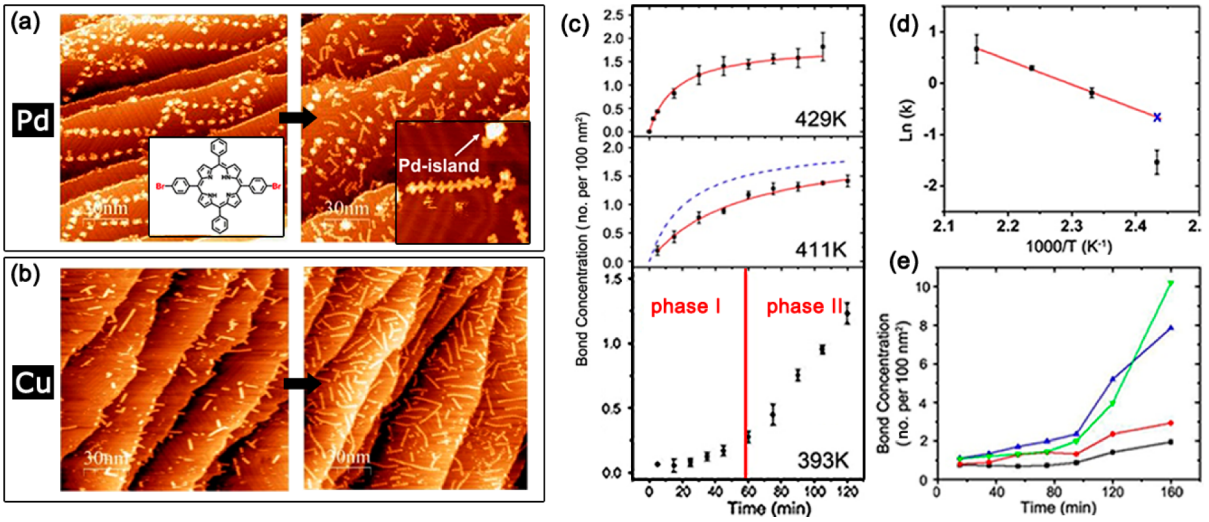

Figure 5. (a) STM images of polymeric chains formed in Pd-activated Ullmann coupling of Br-DPP on Au(111) with annealing to 447 K for 5 min (left) or 105 min (right). Inset, high-resolution STM image of the Br-DPP chain (25 × 25 nm^2). (b) STM images of polymeric chains formed in Cu-activated Ullmann coupling of Br-DPP on Au(111) with annealing to 453 K for 5 min (left) or 160 min (right). (c) Bond concentration in Pd-activated coupling as a function of reaction time at 393, 411, or 429 K. (d) Arrhenius plot of rate constant k obtained from experimental data. (e) Bond concentration in Cu-activated coupling as a function of reaction time at 399 K (black), 417 K (red), 435 K (blue) or 453 K (green). Results at 453 K were scaled down by a factor of 5. Reproduced with permission from ref 53. Copyright 2014 Wiley-VCH.

cleaved when they arrive at the kink sites. Then they remain there due to the high diffusion barrier.

2.4. Extrinsic Atom Activation

The surface-confined Ullmann coupling discussed in the previous sections used *intrinsic* surface atoms or adatoms popping out of the surface to activate the reaction. Surface-confined coupling reactions can also be activated by *extrinsic* foreign metal deposits. In the following, we discuss three extrinsic elements, Pt, Pd, and Cu. Pt is a widely used catalyst.[51] In their study, Dong and Lin deposited Pt on Ag(111) to test Pt activity, taking the advantage of the fact that the Ag surface is known to be poor at activating Ullmann coupling.[47] After depositing TBPB and Pt on Ag(111) and annealing to 320 K, they observed bright dots, which are attributed to Pt atoms, attached at corners of the TBPB molecules (Figure 4a). Figure 4b shows magnified STM topographs highlighting four representative structures formed by TBPB and Pt. Structure II features a TBPB dimer linked via a pronounced protrusion, with a center-to-center distance of 1.74 nm (Figure 4b). Such pronounced protrusions appeared more frequently with increasing Pt dosage. Note that the Ag organometallic TBPB dimers feature a much smaller metal center, as shown in Figure 2a. Thus, the dimer is assigned to an organometallic intermediate containing a C−Pt−C bridge. Pt in these intermediates could coordinate with one to four aryl moieties, as illustrated by the models depicted in Figure 4b. Annealing to 380 K converted 90% of the intermediate structures into covalently linked species, and further annealing to 470 K achieved approximately 100% conversion, indicating that Pt effectively activates the surface-confined Ullmann reaction.

Pd is another versatile catalyst used in a wide range of homo- and cross-coupling reactions.[52] Adisoejoso et al. deposited Pd on a Au(111) surface and examined the Ullmann coupling of 5,15-bis(4-bromo-phenyl)-10,20-diphenyl porphyrin (Br-DPP, inset of Figure 5a) and compared with the results of using Cu on the same surface.[53] Predepositing Pd onto Au(111) and then depositing Br-DPP led to covalently linked polymeric chains at room temperature. Similar polymeric chains were obtained with Cu deposits after 400 K annealing and on bare Au(111) after 450 K annealing. Thus, both Pd and Cu activate the Ullmann coupling. Adisoejoso et al. determined reaction rate constants by monitoring isothermal reaction products *in situ* using STM. C−C bond concentration was measured after annealing to different temperatures for different durations (Figure 5c). In the presence of Pd deposits, bond concentration initially rose rapidly at annealing temperatures above 420 K, then gradually reached saturation; the initial rapid increase was less apparent at annealing temperatures below 420 K. At an even lower temperature of 393 K, a biphasic behavior appeared: a relatively slow increase lasting from 0 to 60 min (phase I) and a rapid increase from 60 to 140 min (phase II). This biphasic

DOI: 10.1021/acs.accounts.5b00160
Acc. Chem. Res. 2015, 48, 2765−2774

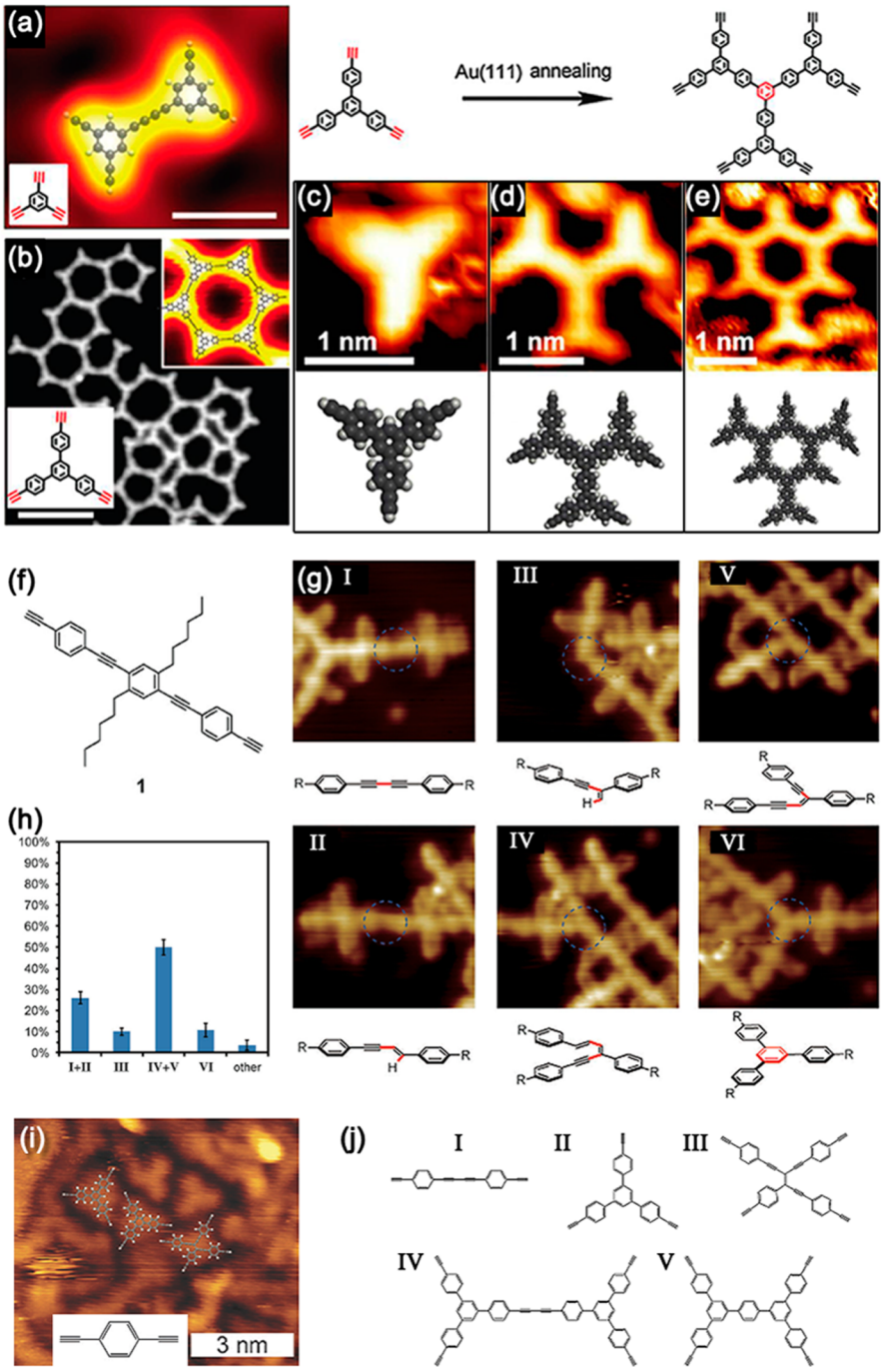

Figure 6. (a, b) Glaser coupling of TEB and Ext-TEB on Ag(111). (a) STM image of a TEB dimer; the calculated dimer structure is superimposed on the image. (b) Covalently bonded networks formed by Ext-TEB. The inset shows a high-resolution image of a hexagon. Scale bars 1 nm. Reproduced with permission from ref 57. Copyright 2012 Nature Publishing Group. (c–e) STM images showing Ext-TEB monomer (c), trimer (d), and hexamer (e) via cyclotrimerization formed on on Au(111), with corresponding molecular models. Reproduced with permission from ref 59. Copyright 2014 Royal Society of Chemistry. (f–h) Glaser coupling and other side reactions of alkyne on Au(111). (f) Chemical structure of diethynylarene. (g) STM images (6×6 nm^2) of six products, each formed by a different reaction pathway. The corresponding molecular structures are shown underneath. (h) Analysis of the relative frequencies of the observed products. Reproduced with permission from ref 60. Copyright 2013 Wiley-VCH. (i) STM image of annealed 1,4-diethynylbenzene monolayers on Cu(111). (j) Structural models of reaction products observed, presumably due to (I) homocoupling, (II) trimerization, (III) cross-coupling, (IV) combined trimerization and homocoupling, or (V) sequential double trimerization. Reproduced with permission from ref 61. Copyright 2013 Royal Society of Chemistry.

behavior suggests the existence of multiple steps in the reaction pathway. Those authors speculated that phase I involves an initial activation process and phase II involves C–C bond formation. The rate-limiting step at higher temperatures is C–C bond formation. The overall rate constant k was determined by fitting the bond concentration using a rate equation. The plot of $\ln(k)$ versus T^{-1} showed a linear relationship for the three reaction temperatures above 420 K (Figure 5d). An activation energy of 0.41 ± 0.03 eV was calculated from the Arrhenius equation. This is much lower than the activation

DOI: 10.1021/acs.accounts.5b00160
Acc. Chem. Res. 2015, 48, 2765–2774

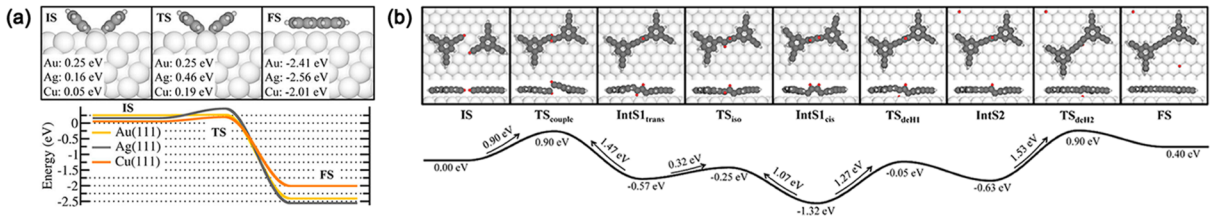

Figure 7. (a) DFT-calculated energy diagram of the second step in Ullmann-type coupling of two phenyls into a biphenyl on Au(111), Ag(111), and Cu(111). In the top panel, the reaction is depicted for Ag(111), with the energy indicated for each of the states along the path on each of the three surfaces. The energies are given with respect to the most stable adsorption configuration of an isolated phenyl on the respective surface. Reproduced with permission from ref 66. Copyright 2013 American Chemical Society. (b) DFT-calculated reaction pathway of Glaser-type coupling and subsequent dehydrogenation of two TEB molecules on a Ag(111) surface. Reproduced with permission from ref 69. Copyright 2014 American Chemical Society.

energy of 1.12 eV reported for the Ullmann coupling of iodobenzene on Cu(111).[54] Besides activation energy, Cu and Pd differ in several other respects: Yields in the Cu-activated reaction do not show saturation and are much higher than those in the Pd-activated ones (Figure 5e). The Cu-activated reaction generates much longer polymeric chains than the Pd-activated process (Figure 5, panel a versus b). These differences hint that Pd lowers the energy barrier of the initial dehalogenation step, whereas Cu lowers the activation energy of subsequent step(s) in the reaction.

3. ALKYNE–ALKYNE (GLASER-TYPE COUPLING)

Glaser coupling is a classic organic reaction that links acetylenes into biynes via cuprous ion-activated oxidative coupling.[55,56] Surface-confined Glaser-type coupling has been achieved on Ag(111), Au(111), and Cu(111). While surface-confined Ullmann-type coupling leaves halogen atoms adsorbed on the surface, surface-confined Glaser coupling generates bisethynylarene products and hydrogen as the only byproduct.

Zhang et al. reported the first example of surface-confined coupling of alkynes on a Ag(111) surface.[57] Thermal annealing of 1,3,5-triethynylbenzene (TEB) up to 330 K resulted in dimerization via Glaser coupling (Figure 6a). The covalent nature of the products was confirmed by DFT simulation and STM manipulation. Under the same conditions, the larger molecule 1,3,5-tris(4-ethynylphenyl)benzene (Ext-TEB) was coupled to form 2D conjugated networks (Figure 6b). Detailed analysis of the binding motifs showed that two competing reaction pathways dominate the coupling process. The first is the Glaser coupling of two alkyne termini, leading to a linear butadiyne bridge. The second is the connection of a butadiyne group to a laterally attacking terminal alkyne. Since this converts the attacked ethyne to ethene moieties, it inhibits the production of regular networks.[58] Interestingly, Liu et al. demonstrated that cyclotrimerization is the dominant reaction pathway for Ext-TEB on a Au(111) surface (Figure 6c–e).[57] Figure 6d and e show after annealing to 373 K, discrete trimers and hexamers formed. The trimers and hexamers arose from cyclotrimerization of three and six TEB molecules, respectively. Further annealing to 433 K resulted in a fully interconnected 2D network via cyclotrimerization. The cyclotrimerization occurred at modest temperatures, starting at around 373 K and proceeding to completion at 433 K, implying that the Au surface activates the reaction.

Gao et al. reported that on Au(111) diethynylarenes (Figure 6f) proceeded in various reaction pathways,[60] including Glaser coupling (Figure 6g, pathway I), formal hydroalkynylation of the terminal alkyne functionality at either the α- or β-position (Figure 6g, pathways II and III), formation of dienyne products (Figure 6g, pathway IV), and hydroalkynylation leading to an enediyne moiety (Figure 6g, pathway V). Alkyne trimerization was also observed, generating a branching point with an aromatic core structure (Figure 6g, pathway VI). Analysis of the relative frequencies of occurrence of these reaction pathways (Figure 6h) showed that pathways I and II, in which the Glaser coupling is the main process, occurred 26% ± 3% of the time, while trimerization occurred 10.7% ± 3.1% of the time. Other researchers have also observed surface-confined diyne polycyclotrimerization on Au(111) via a two-step [2 + 2 + 2] cyclization reaction.[62]

Eichhorn et al. examined surface-confined coupling reaction of 1,4-diethynyklbenzene on Cu(111). Thermally disordered covalent aggregates and networks formed after annealing the sample to 573 K (Figure 6i).[61] Structural analysis of these structures suggested the simultaneous occurrence of several side reactions other than Glaser coupling, including trimerization, cross-coupling, combined trimerization and homocoupling, and sequential double trimerization (Figure 6j). These reaction pathways could not be controlled by changing the annealing temperature or time.

The different products formed on different surfaces clearly demonstrate that the surface-confined Glaser-type coupling is surface sensitive. Using 1,4-diethynyl-benzene as a model system, Gao et al. compared the surface-confined Glaser coupling on Au(111), Ag(111), and Cu(111).[63] Analysis of the frequencies of bond-forming events showed that Ag led to a lower proportion of byproducts than Au, while the coupling was quite inefficient on Cu(111). DFT calculations suggest a mechanistic model in which the alkyne functionality interacts with the Au or Ag surface and direct C–C bond formation is the rate-determining step. In conclusion, Ag is more efficient than Au or Cu for Glaser-type coupling, which differs from the trend found in the surface-confined Ullmann-type reaction.

Two strategies have been demonstrated to improve chemoselectivity of surface-confined Glaser-type coupling. One is to block one *ortho* position next to the reacting alkyne moiety using an alkyl substituent. This side group reduces or entirely eliminates side reactions for steric reasons, making Glaser-type coupling the major reaction pathway. Another strategy is to use a vicinal surface. On a Ag(877) surface, which has narrow terraces, homocoupling of 1,4-diethynylbenzene resulted in extended graphdiyne wires with lengths reaching 30 nm.[64]

4. COMPUTATIONAL STUDIES

Computational studies can provide detailed atomistic insights into the reaction mechanisms including reaction paths, energy

DOI: 10.1021/acs.accounts.5b00160
Acc. Chem. Res. 2015, 48, 2765–2774

barrier, rate-limiting steps, and intermediate and transition states.[65] These studies may be carried out for various interesting metal surfaces and molecules with selected reaction groups, which can reveal comparative trends for the same reactions taking place on different surfaces. DFT with correct functionals is one of the most powerful and reliable tools to obtain equilibrium structures. The transition-state calculations, however, are much more challenging and resource demanding due to the large size of the systems. Here we select two examples to show the typical outcomes of using DFT to study surface-confined coupling reactions.

Bjork et al. performed DFT-based transition-state calculations to compare the reaction barriers of Ullmann-type coupling of two bromobenzene molecules on (111) surfaces of Au, Ag, and Cu.[66] The calculations found the reaction consists of two steps: (1) dehalogenation forming surface-supported radicals (**IS**) and (2) coupling of two **IS** to a biphenyl (**FS**). It was found that the barrier for halogen dissociation is reduced from 3.9 eV in vacuum to 1.0, 0.8, and 0.7 eV on Au(111), Ag(111), and Cu(111), respectively. The second step is highly exothermic on all three surfaces (Figure 7a). On Au(111), the barrier separating the **IS** and **FS** is below the 0.01 eV resolution of the calculations, but 0.25 eV is required to bring two well-separated phenyls to the **IS**. On Cu(111), the barrier is also rather small, while it is greatest on Ag(111). However, the reaction pathway involving the organometallic intermediate state has not been reported. It is worthwhile to note that the reaction pathway and mechanism of Ullmann-type coupling between large precursor molecules such as 4,4′-dibromo-*p*-terphenyl or TBPB most likely differ from the small bromobenzene since the large molecules are expected to be adsorbed differently from the **IS** shown in Figure 7a.

Glaser-type coupling in solution is known to proceed via a Cu−acetylide intermediate, generated from dehydrogenation of the terminal alkyne with a copper ion.[67] In the presence of Ag ions, a Ag−acetylide intermediate can form.[68] The mechanism of surface-confined Glaser-type coupling, in contrast, is poorly understood. Characterization of TEB dimerization on Ag(111) using XPS and DFT calculations excluded a potential organometallic intermediate state.[57] DFT-based transition state calculations suggest that surface-confined Glaser-type coupling is initiated by covalent coupling between two molecules instead of by single-molecule dehydrogenation. Figure 7b shows that two TEB molecules first form a dimer intermediate and then undergo two rate-limiting dehydrogenation processes to afford the diyne.[69] Ag(111) stabilizes the coupled intermediate prior to dehydrogenation, as well as constrains the molecular motion to two dimensions. DFT also suggested that direct covalent bond formation followed by step-by-step dissociation of two hydrogen atoms has a lower activation barrier than formation of an organometallic Ag bis-acetylide complex.

5. CONCLUSION AND OUTLOOK

In this Account, we have reviewed the surface-confined coupling reactions of aryl−halogen (Ullmann-type) and alkyne (Glaser-type) on the (111) surfaces of Cu, Ag, and Au. In comparison, the surface-confined Ullmann-type coupling is better understood, while the Glaser-type coupling is more intricate. Both types of reactions are sensitive to the surface, but in different manners. Aryl−halogens yield the same products featuring an aryl−aryl bond regardless of the choice of the surface. Nevertheless, the reaction intermediate is surface sensitive: an organometallic intermediate forms on Cu and Ag but not on Au. The surface activity is in the order of Au > Cu > Ag. The reaction barrier can be further reduced using the extrinsic element of Pt or Pd. Alkynes, in contrast, yield different products, depending on the surface. Glaser-type coupling is by far the predominant reaction on Ag(111), whereas appreciable amounts of byproducts are unavoidable on Au(111) and Cu(111). Under certain conditions, cyclotrimerization prevails on Au(111). Surface activity varies in the order of Ag > Au > Cu. No organometallic intermediate was observed on any of the surfaces. In both reactions, surface morphology, including narrow terraces and kinks, were found to be able to steer the reactions. In summary, both types of coupling reactions can proceed on the noble metal surfaces but exhibit distinctive features: Ullmann-type coupling results in single products; in contrast, Glaser-type coupling results in multiple products. The drawback of Ullmann-type coupling is that the residual Br atoms very often interfere with or even hinder the reaction, while Glaser-type coupling is cleaner with H as the byproduct.

The results reviewed in this Account, however, raise more questions than providing answers. Despite the progress made so far, the pathway of the surface-confined coupling reactions and the mechanism of the surface activation are largely unknown. For example, it is mystery why Glaser coupling proceeds on Ag(111) but cyclotrimerization results on Au(111) for the same reactant molecule. We end this Account with a list of questions and perspectives for future work in this field: By what steps does the organometallic intermediate form in the Ullmann coupling? How does the charge state of the metal atoms change in the reactions? How can we make use of specific molecular conformation upon surface adsorption to yield target products but block side reactions? Is it feasible to make use of surface chirality to achieve chiral-selected surface-confined coupling reactions? Can other textbook couplings, in particular, cross-coupling, be realized on surface and if so how? Joint efforts made by synthetic chemists, surface scientists, and theorists targeting specific model systems are hopeful to answer these questions. Satisfactory answers to these questions will shed light on the design principle for forming large area defect-free 2D ordered nanostructures using surface-confined coupling reactions.

AUTHOR INFORMATION

Corresponding Authors

*E-mail: phnlin@ust.hk.
*E-mail: liupn@ecust.edu.cn.

Funding

This work was supported by Hong Kong RGC 603213 and NSFC (Nos. 21421004 and 21190033).

Notes

The authors declare no competing financial interest.

Biographies

Lei Dong received a B.S degree in applied physics in 2004 from University of Science and Technology of China, and currently he is a research assistant at Hong Kong University of Science and Technology focusing on fundamental studies of surfaces and catalysis.

Pei Nian Liu obtained his Ph.D. in 2004 from the Chemistry Department at Lanzhou University. He then worked for four years as a Research Associate in the Chemistry Department at the Hong Kong

DOI: 10.1021/acs.accounts.5b00160
Acc. Chem. Res. 2015, 48, 2765−2774

University of Science and Technology and as a Postdoctoral Fellow in the Department of Applied Biology and Chemical Technology at the Hong Kong Polytechnic University. He joined East China University of Science and Technology as Associate Professor in 2008, and was promoted to Professor in 2012. He was appointed Eastern Scholar Distinguished Professor in 2015. His research interests include on-surface organic reactions investigated by UHV-STM and catalytic organic reactions in solution.

Nian Lin earned his Ph.D. at the Hong Kong University of Science and Technology in 1997. He was a postdoctoral researcher from 1997 to 1999 in Linkoping University, Sweden. From 2000 to 2007, he was working in the group of Prof. Klaus Kern at the Max-Planck-Institute for Solid State Research in Stuttgart, Germany. Since 2007, he joined the Physics Department of the Hong Kong University of Science and Technology, first as an Associate Professor and since 2014 as a Full Professor. His research focuses on applying surface-confined supramolecular self-assembly and covalent coupling to design low-dimensional macromolecular and supramolecular structures, and using scanning tunneling microscopy and spectroscopy to characterize these structures.

REFERENCES

(1) Zwaneveld, N. A. A.; Pawlak, R.; Abel, M.; Catalin, D.; Gigmes, D.; Bertin, D.; Porte, L. Organized Formation of 2D Extended Covalent Organic Frameworks at Surfaces. *J. Am. Chem. Soc.* **2008**, *130*, 6678−6679.

(2) Ourdjini, O.; Pawlak, R.; Abel, M.; Clair, S.; Chen, L.; Bergeon, N.; Sassi, M.; Oison, V.; Debierre, J.-M.; Coratger, R.; Porte, L. Substrate-Mediated Ordering and Defect Analysis of a Surface Covalent Organic Framework. *Phys. Rev. B: Condens. Matter Mater. Phys.* **2011**, *84*, 125421.

(3) Dienstmaier, J. F.; Medina, D. D.; Dogru, M.; Knochel, P.; Bein, T.; Heckl, W. M.; Lackinger, M. Isoreticular Two-Dimensional Covalent Organic Frameworks Synthesized by on-surface Condensation of Diboronic Acids. *ACS Nano* **2012**, *6*, 7234−7242.

(4) Weigelt, S.; Bombis, C.; Busse, C.; Knudsen, M. M.; Gothelf, K. V.; Lægsgaard, E.; Besenbacher, F.; Linderoth, T. R. Molecular Self-Assembly from Building Blocks Synthesized on a Surface in Ultrahigh Vacuum: Kinetic Control and Topo-Chemical Reactions. *ACS Nano* **2008**, *2*, 651−660.

(5) Matena, M.; Riehm, T.; Stöhr, M.; Jung, T. A.; Gade, L. H. Transforming Surface Coordination Polymers into Covalent Surface Polymers: Linked Polycondensed Aromatics through Oligomerization of N-Heterocyclic Carbene Intermediates. *Angew. Chem.* **2008**, *120*, 2448−2451.

(6) Zhong, D.; Franke, J.-H.; Podiyanachari, S. K.; Blömker, T.; Zhang, H.; Kehr, G.; Erker, G.; Fuchs, H.; Chi, L. Linear Alkane Polymerization on a Gold Surface. *Science* **2011**, *334*, 213−216.

(7) Treier, M.; Richardson, N. V.; Fasel, R. Fabrication of Surface-Supported Low-Dimensional Polyimide Networks. *J. Am. Chem. Soc.* **2008**, *130*, 14054−14055.

(8) Marele, A. C.; Mas-Ballesté, R.; Terracciano, L.; Rodríguez-Fernández, J.; Berlanga, I.; Alexandre, S. S.; Otero, R.; Gallego, J. M.; Zamora, F.; Gómez-Rodríguez, J. M. Formation of a Surface Covalent Organic Framework Based on Polyester Condensation. *Chem. Commun.* **2012**, *48*, 6779−6781.

(9) Sun, Q.; Zhang, C.; Li, Z.; Kong, H.; Tan, Q.; Hu, A.; Xu, W. On-Surface Formation of One-Dimensional Polyphenylene through Bergman Cyclization. *J. Am. Chem. Soc.* **2013**, *135*, 8448−8451.

(10) Treier, M.; Pignedoli, C. A.; Laino, T.; Rieger, R.; Müllen, K.; Passerone, D.; Fasel, R. Surface-Assisted Cyclodehydrogenation Provides a Synthetic Route Towards Easily Processable and Chemically Tailored Nanographenes. *Nat. Chem.* **2011**, *3*, 61−67.

(11) Otero, G.; Biddau, G.; Sánchez-Sánchez, C.; Caillard, R.; López, M. F.; Rogero, C.; Palomares, F. J.; Cabello, N.; Basanta, M. A.; Ortega, J.; Méndez, J.; Echavarren, A. M.; Pérez, R.; Gómez-Lor, B.; Martín-Gago, J. A. Fullerenes from Aromatic Precursors by Surface-Catalysed Cyclodehydrogenation. *Nature* **2008**, *454*, 865−868.

(12) Bebensee, F.; Bombis, C.; Vadapoo, S.-R.; Cramer, J. R.; Besenbacher, F.; Gothelf, K. V.; Linderoth, T. R. On-Surface Azide−Alkyne Cycloaddition on Cu(111): Does It "Click" in Ultrahigh Vacuum? *J. Am. Chem. Soc.* **2013**, *135*, 2136−2139.

(13) Díaz Arado, O.; Mönig, H.; Wagner, H.; Franke, J.-H.; Langewisch, G.; Held, P. A.; Studer, A.; Fuchs, H. On-Surface Azide−Alkyne Cycloaddition on Au(111). *ACS Nano* **2013**, *7*, 8509−8515.

(14) Franc, G.; Gourdon, A. Covalent Networks through on-Surface Chemistry in Ultra-High Vacuum: State-of-the-Art and Recent Developments. *Phys. Chem. Chem. Phys.* **2011**, *13*, 14283−14292.

(15) El Garah, M.; MacLeod, J. M.; Rosei, F. Covalently Bonded Networks Through Surface-Confined Polymerization. *Surf. Sci.* **2013**, *613*, 6−14.

(16) Lackinger, M.; Heckl, W. M. A STM Perspective on Covalent Intermolecular Coupling Reactions on Surfaces. *J. Phys. D: Appl. Phys.* **2011**, *44*, 464011.

(17) Méndez, J.; Lopez, M. F.; Martín-Gago, J. A. On-Surface Synthesis of Cyclic Organic Molecules. *Chem. Soc. Rev.* **2011**, *40*, 4578−4590.

(18) Ullmann, F.; Bielecki, J. Ueber Synthesen in Der Biphenylreihe. *Ber. Dtsch. Chem. Ges.* **1901**, *34*, 2174−2185.

(19) Sambiagio, C.; Marsden, S. P.; Blacker, A. J.; McGowan, P. C. Copper Catalysed Ullmann Type Chemistry: From Mechanistic Aspects to Modern Development. *Chem. Soc. Rev.* **2014**, *43*, 3525−3550.

(20) Xi, M.; Bent, B. E. Iodobenzene on Cu(111): Formation and Coupling of Adsorbed Phenyl Groups. *Surf. Sci.* **1992**, *278*, 19−32.

(21) Xi, M.; Bent, B. E. Mechanisms of the Ullmann Coupling Reaction in Adsorbed Monolayers. *J. Am. Chem. Soc.* **1993**, *115*, 7426−7433.

(22) Hla, S.-W.; Bartels, L.; Meyer, G.; Rieder, K.-H. Inducing All Steps of a Chemical Reaction with the Scanning Tunneling Microscope Tip: Towards Single Molecule Engineering. *Phys. Rev. Lett.* **2000**, *85*, 2777−2780.

(23) Grill, L.; Dyer, M.; Lafferentz, L.; Persson, M.; Peters, M. V.; Hecht, S. Nano-Architectures by Covalent Assembly of Molecular Building Blocks. *Nat. Nanotechnol.* **2007**, *2*, 687−691.

(24) Wang, W.; Shi, X.; Wang, S.; Van Hove, M. A.; Lin, N. Single-Molecule Resolution of an Organometallic Intermediate in a Surface-Supported Ullmann Coupling Reaction. *J. Am. Chem. Soc.* **2011**, *133*, 13264−13267.

(25) Walch, H.; Gutzler, R.; Sirtl, T.; Eder, G.; Lackinger, M. Material- and Orientation-Dependent Reactivity for Heterogeneously Catalyzed Carbon−Bromine Bond Homolysis. *J. Phys. Chem. C* **2010**, *114*, 12604−12609.

(26) Gutzler, R.; Walch, H.; Eder, G.; Kloft, S.; Heckl, W. M.; Lackinger, M. Surface Mediated Synthesis of 2D Covalent Organic Frameworks: 1,3,5-Tris(4-Bromophenyl)Benzene on Graphite (001), Cu (111), and Ag (110). *Chem. Commun.* **2009**, *0*, 4456−4458.

(27) Blake, M. M.; Nanayakkara, S. U.; Claridge, S. A.; Fernández-Torres, L. C.; Sykes, E. C. H.; Weiss, P. S. Identifying Reactive Intermediates in the Ullmann Coupling Reaction by Scanning Tunneling Microscopy and Spectroscopy. *J. Phys. Chem. A* **2009**, *113*, 13167−13172.

(28) Chung, K.-H.; Koo, B.-G.; Kim, H.; Yoon, J. K.; Kim, J.-H.; Kwon, Y.-K.; Kahng, S.-J. Electronic Structures of One-Dimensional Metal-Molecule Hybrid Chains Studied Using Scanning Tunneling Microscopy and Density Functional Theory. *Phys. Chem. Chem. Phys.* **2012**, *14*, 7304−7308.

(29) Russell, J. C.; Blunt, M. O.; Garfitt, J. M.; Scurr, D. J.; Alexander, M.; Champness, N. R.; Beton, P. H. Dimerization of Tri(4-Bromophenyl)Benzene by Aryl−Aryl Coupling from Solution on a Gold Surface. *J. Am. Chem. Soc.* **2011**, *133*, 4220−4223.

(30) Cai, J.; Ruffieux, P.; Jaafar, R.; Bieri, M.; Braun, T.; Blankenburg, S.; Muoth, M.; Seitsonen, A. P.; Saleh, M.; Feng, X.; Müllen, K.; Fasel, R. Atomically Precise Bottom-Up Fabrication of Graphene Nanoribbons. *Nature* **2010**, *466*, 470−473.

DOI: 10.1021/acs.accounts.5b00160
Acc. Chem. Res. 2015, 48, 2765−2774

(31) Lafferentz, L.; Eberhardt, V.; Dri, C.; Africh, C.; Comelli, G.; Esch, F.; Hecht, S.; Grill, L. Controlling On-Surface Polymerization by Hierarchical and Substrate-Directed Growth. *Nat. Chem.* **2012**, *4*, 215−220.
(32) Fan, Q.; Wang, C.; Han, Y.; Zhu, J.; Hieringer, W.; Kuttner, J.; Hilt, G.; Gottfried, J. M. Surface-Assisted Organic Synthesis of Hyperbenzene Nanotroughs. *Angew. Chem., Int. Ed.* **2013**, *52*, 4668−4672.
(33) Chen, M.; Xiao, J.; Steinrück, H.-P.; Wang, S.; Wang, W.; Lin, N.; Hieringer, W.; Gottfried, J. M. Combined Photoemission and Scanning Tunneling Microscopy Study of the Surface-Assisted Ullmann Coupling Reaction. *J. Phys. Chem. C* **2014**, *118*, 6820−6830.
(34) Fan, Q.; Wang, C.; Liu, L.; Han, Y.; Zhao, J.; Zhu, J.; Kuttner, J.; Hilt, G.; Gottfried, J. M. Covalent, Organometallic, and Halogen-Bonded Nanomeshes from Tetrabromo-Terphenyl by Surface-Assisted Synthesis on Cu(111). *J. Phys. Chem. C* **2014**, *118*, 13018−13025.
(35) Fan, Q.; Wang, C.; Han, Y.; Zhu, J.; Kuttner, J.; Hilt, G.; Gottfried, J. M. Surface-Assisted Formation, Assembly, and Dynamics of Planar Organometallic Macrocycles and Zigzag Shaped Polymer Chains with C−Cu−C Bonds. *ACS Nano* **2014**, *8*, 709−718.
(36) Yang, M. X.; Xi, M.; Yuan, H.; Bent, B. E.; Stevens, P.; White, J. M. NEXAFS Studies of Halobenzenes and Phenyl Groups on Cu(111). *Surf. Sci.* **1995**, *341*, 9−18.
(37) Fanta, P. E. The Ullmann Synthesis of Biaryls; Synthesis. *Chem. Rev.* **1946**, *38*, 139−196.
(38) Cohen, T.; Cristea, I. Kinetics and Mechanism of the Copper(I)-Induced Homogeneous Ullmann Coupling of O-Bromonitrobenzene. *J. Am. Chem. Soc.* **1976**, *98*, 748−753.
(39) Bieri, M.; Nguyen, M.-T.; Gröning, O.; Cai, J.; Treier, M.; Aït-Mansour, K.; Ruffieux, P.; Pignedoli, C. A.; Passerone, D.; Kastler, M.; Müllen, K.; Fasel, R. Two-Dimensional Polymer Formation on Surfaces: Insight into the Roles of Precursor Mobility and Reactivity. *J. Am. Chem. Soc.* **2010**, *132*, 16669−16676.
(40) Lipton−Duffin, J. A.; Ivasenko, O.; Perepichka, D. F.; Rosei, F. Synthesis of Polyphenylene Molecular Wires by Surface-Confined Polymerization. *Small* **2009**, *5*, 592−597.
(41) McCarty, G. S.; Weiss, P. S. Formation and Manipulation of Protopolymer Chains. *J. Am. Chem. Soc.* **2004**, *126*, 16772−16776.
(42) Nguyen, M.-T.; Pignedoli, C. A.; Passerone, D. An Ab Initio Insight into the Cu(111)-Mediated Ullmann Reaction. *Phys. Chem. Chem. Phys.* **2011**, *13*, 154−160.
(43) Lewis, E. A.; Murphy, C. J.; Liriano, M. L.; Sykes, E. C. H. Atomic-Scale Insight into the Formation, Mobility and Reaction of Ullmann Coupling Intermediates. *Chem. Commun.* **2014**, *50*, 1006−1008.
(44) Park, J.; Kim, K. Y.; Chung, K.-H.; Yoon, J. K.; Kim, H.; Han, S.; Kahng, S.-J. Interchain Interactions Mediated by Br Adsorbates in Arrays of Metal-Organic Hybrid Chains on Ag(111). *J. Phys. Chem. C* **2011**, *115*, 14834−14838.
(45) Di Giovannantonio, M.; El Garah, M.; Lipton-Duffin, J.; Meunier, V.; Cardenas, L.; Revurat, Y. F.; Cossaro, A.; Verdini, A.; Perepichka, D. F.; Rosei, F.; Contini, G. Insight into Organometallic Intermediate and Its Evolution to Covalent Bonding in Surface-Confined Ullmann Polymerization. *ACS Nano* **2013**, *7*, 8190−8198.
(46) Blunt, M. O.; Russell, J. C.; Champness, N. R.; Beton, P. H. Templating Molecular Adsorption Using a Covalent Organic Framework. *Chem. Commun.* **2010**, *46*, 7157−7159.
(47) Dong, L.; Lin, N. *On-Surface Synthesis*; Advances in Atom and Single Molecule Machines; Springer: Dordrecht, the Netherlands, **2015**, in press.
(48) Koch, M.; Gille, M.; Viertel, A.; Hecht, S.; Grill, L. Substrate-Controlled Linking of Molecular Building Blocks: Au(111) vs. Cu(111). *Surf. Sci.* **2014**, *627*, 70−74.
(49) Gutzler, R.; Cardenas, L.; Lipton-Duffin, J.; El Garah, M.; Dinca, L. E.; Szakacs, C. E.; Fu, C.; Gallagher, M.; Vondráček, M.; Rybachuk, M.; Perepichka, D. F.; Rosei, F. Ullmann-Type Coupling of Brominated Tetrathienoanthracene on Copper and Silver. *Nanoscale* **2014**, *6*, 2660−2668.
(50) Saywell, A.; Schwarz, J.; Hecht, S.; Grill, L. Polymerization on Stepped Surfaces: Alignment of Polymers and Identification of Catalytic Sites. *Angew. Chem.* **2012**, *124*, 5186−5190.
(51) Wintterlin, J.; Völkening, S.; Janssens, T.; Zambelli, T.; Ertl, G. Atomic and Macroscopic Reaction Rates of a Surface-Catalyzed Reaction. *Science* **1997**, *278*, 1931−1934.
(52) Molnár, A. Efficient, Selective, and Recyclable Palladium Catalysts in Carbon− Carbon Coupling Reactions. *Chem. Rev.* **2011**, *111*, 2251−2320.
(53) Adisoejoso, J.; Lin, T.; Shang, X. S.; Shi, K. J.; Gupta, A.; Liu, P. N.; Lin, N. A Single-Molecule-Level Mechanistic Study of Pd-Catalyzed and Cu-Catalyzed Homocoupling of Aryl Bromide on an Au(111) Surface. *Chem. - Eur. J.* **2014**, *20*, 4111−4116.
(54) Meyers, J. M.; Gellman, A. J. Effect of Substituents on the Phenyl Coupling Reaction on Cu(111). *Surf. Sci.* **1995**, *337*, 40−50.
(55) Glaser, C. Beiträge Zur Kenntniss Des Acetenylbenzols. *Ber. Dtsch. Chem. Ges.* **1869**, *2*, 422−424.
(56) Hay, A. S. Oxidative Coupling of Acetylenes. II 1. *J. Org. Chem.* **1962**, *27*, 3320−3321.
(57) Zhang, Y. Q.; Kepčija, N.; Kleinschrodt, M.; Diller, K.; Fischer, S.; Papageorgiou, A. C.; Allegretti, F.; Björk, J.; Klyatskaya, S.; Klappenberger, F.; Ruben, M.; Barth, J. V. Homo-Coupling of Terminal Alkynes on a Noble Metal Surface. *Nat. Commun.* **2012**, *3*, 1286.
(58) Cirera, B.; Zhang, Y. Q.; Klyatskaya, S.; Ruben, M.; Klappenberger, F.; Barth, J. V. 2 D Self-Assembly and Catalytic Homo-Coupling of the Terminal Alkyne 1,4-Bis(3,5-Diethynyl-Phenyl)Butadiyne-1,3 on Ag(111). *ChemCatChem* **2013**, *5*, 3281−3288.
(59) Liu, J.; Ruffieux, P.; Feng, X.; Müllen, K.; Fasel, R. Cyclotrimerization of Arylalkynes on Au (111). *Chem. Commun.* **2014**, *50*, 11200−11203.
(60) Gao, H. Y.; Wagner, H.; Zhong, D.; Franke, J.-H.; Studer, A.; Fuchs, H. Glaser Coupling at Metal Surfaces. *Angew. Chem., Int. Ed.* **2013**, *52*, 4024−4028.
(61) Eichhorn, J.; Heckl, W. M.; Lackinger, M. On-surface Polymerization of 1,4-Diethynylbenzene on Cu(111). *Chem. Commun.* **2013**, *49*, 2900−2902.
(62) Gao, H. Y.; Zhong, D.; Mönig, H.; Wagner, H.; Held, P.-A.; Timmer, A.; Studer, A.; Fuchs, H. Photochemical Glaser Coupling at Metal Surfaces. *J. Phys. Chem. C* **2014**, *118*, 6272−6277.
(63) Gao, H. Y.; Franke, J.-H.; Wagner, H.; Zhong, D.; Held, P.-A.; Studer, A.; Fuchs, H. Effect of Metal Surfaces in On-Surface Glaser Coupling. *J. Phys. Chem. C* **2013**, *117*, 18595−18602.
(64) Cirera, B.; Zhang, Y. Q.; Björk, J.; Klyatskaya, S.; Chen, Z.; Ruben, M.; Barth, J. V.; Klappenberger, F. Synthesis of Extended Graphdiyne Wires by Vicinal Surface Templating. *Nano Lett.* **2014**, *14*, 1891−1897.
(65) Björk, J.; Hanke, F. Towards Design Rules for Covalent Nanostructures on Metal Surfaces. *Chem. - Eur. J.* **2014**, *20*, 928−934.
(66) Björk, J.; Hanke, F.; Stafström, S. Mechanisms of Halogen-Based Covalent Self-Assembly on Metal Surfaces. *J. Am. Chem. Soc.* **2013**, *135*, 5768−5775.
(67) Siemsen, P.; Livingston, R. C.; Diederich, F. Acetylenic Coupling: A Powerful Tool in Molecular Construction. *Angew. Chem., Int. Ed.* **2000**, *39*, 2632−2657.
(68) Halbes-Letinois, U.; Weibel, J.-M.; Pale, P. The Organic Chemistry of Silver Acetylides. *Chem. Soc. Rev.* **2007**, *36*, 759−769.
(69) Björk, J.; Zhang, Y. Q.; Klappenberger, F.; Barth, J. V.; Stafström, S. Unraveling the Mechanism of the Covalent Coupling Between Terminal Alkynes on a Noble Metal. *J. Phys. Chem. C* **2014**, *118*, 3181−3187.

DOI: 10.1021/acs.accounts.5b00160
Acc. Chem. Res. 2015, 48, 2765−2774